Human Reproduction, Vol.34, No.3 pp. 452–468, 2019
Advanced Access publication on January 28, 2019 doi:10.1093/humrep/dey392

human reproduction

ORIGINAL ARTICLE *Gynaecology*

Sensory nerve-derived neuropeptides accelerate the development and fibrogenesis of endometriosis

Xishi Liu[1,2,†], Dingmin Yan[1,†], and Sun-Wei Guo[1,2,*]

[1]Shanghai OB/GYN Hospital, Fudan University, Shanghai 200011, China [2]Shanghai Key Laboratory of Female Reproductive Endocrine-Related Diseases, Fudan University, Shanghai, China

*Correspondence address. Research Institute, Shanghai OB/GYN Hospital, Fudan University, 419 Fangxie, Shanghai 200011, China. E-mail: hoxa10@outlook.com

Submitted on July 27, 2018; resubmitted on December 4, 2018; accepted on December 14, 2018

STUDY QUESTION: Do sensory nerves play any role in the development of endometriosis?

SUMMARY ANSWER: Sensory nerves participate in all major steps (epithelial–mesenchymal transition (EMT), fibroblast-to-myofibroblast transdifferentiation (FMT) and smooth muscle metaplasia (SMM)) in the development and fibrogenesis of endometriotic lesions.

WHAT IS KNOWN ALREADY: Endometriotic lesions are known to be hyperinnervated due to neurogenesis resulting from neutrophins secreted by endometriotic lesions and possibly platelets. These neutrophins seem to preferentially favour production of sensory neurons at the expense of sympathetic neurons.

STUDY DESIGN, SIZE, DURATION: Three independent, yet complementary, prospective, randomized mouse experimentations were conducted. A total of 143 female Balb/C mice and 24 female immunodeficient nude Balb/C mice were used. The mice were sacrificed 2 or 4 weeks after the induction of endometriosis.

PARTICIPANTS/MATERIALS, SETTING, METHODS: In Experiment 1, 21 mice were randomly divided into three groups of equal size for sympathetic denervation, sensory denervation and controls. Denervation was carried out chemically. In Experiment 2, 24 nude mice were randomly divided into three equal-sized groups: the BEFORE and AFTER groups that respectively received surgical denervation 3 days before or after the induction of endometriosis by subcutaneous grafting of human endometriotic tissues, and the Control group that received a sham surgery without denervation 3 days before induction. For Experiments 1 and 2, all mice were sacrificed two weeks after induction of endometriosis. In Experiment 3, substance P (SP) and aprepitant, a potent and selective neurokinin 1 receptor (NK1R) antagonist, were used to activate and inhibit the NK1R signalling pathway, respectively. A total of 32 mice were randomly divided into four groups of equal sizes: control (CTL), SP, Before-Induction and After-Induction. One day before the induction of endometriosis, mice in CTL, SP and Before-Induction groups were infused with sterile saline, SP and aprepitant, respectively, via Alzet osmotic pumps. Two weeks after the induction, the After-induction group was infused with aprepitant in similar fashion. All mice were sacrificed four weeks after the induction of endometriosis. In all three experiments, the bodyweight and hotplate latency were evaluated before induction and sacrifice. In addition, all lesions were excised, weighed and processed for quantification and immunohistochemistry analysis of markers for EMT, FMT and SMM, and the extent of fibrosis was evaluated by Masson trichrome staining.

MAIN RESULTS AND THE ROLE OF CHANCE: In Experiment 1, chemical denervation of sympathetic and sensory nerves reduced the lesion weight by 43.2% (±23.1%) and 68.7% (±20.3%), respectively, as compared with controls. In particular, sensory denervation led to significantly greater reduction in lesion weight than sympathetic denervation. Sensory denervation also resulted in significantly improved hyperalgesia as compared with controls. In contrast, sympathetic denervation yielded only transient improvement in hyperalgesia. Both sympathetic and sensory denervation resulted in lower immunoreactivity against markers of proliferation and fibrosis, especially sensory denervation.

In Experiment 2, surgical denervation before or after induction of endometriosis also decelerated the development of endometriosis, as manifested by significantly reduced lesion weight and extent of lesional fibrosis, along with improved hyperalgesia.

[†]These two authors contributed equally to this work.

In Experiment 3, NK1R activation by SP infusion accelerated lesional development, as evidenced by significantly increased lesional weight, more thorough progression of EMT, FMT, SMM, exaggerated lesional fibrosis and deteriorated hyperalgesia. In contrast, NK1R antagonism decelerated lesional development and improved hyperalgesia.

LARGE SCALE DATA: N/A.

LIMITATIONS, REASONS FOR CAUTION: This study is limited by the use of histologic and immunohistochemistry analyses only and the lack of molecular data.

WIDER IMPLICATIONS OF THE FINDINGS: Since sensory nerves are known to be important in wound healing and fibrogenesis, our findings also give more credence to the notion that endometriotic lesions are wounds undergoing repeated tissue injury and repair. As such, sensory nerves or the NK1R signalling pathway in particular may be potential targets for intervention.

STUDY FUNDING/COMPETING INTEREST(S): This research was supported by Grants 81471434 (SWG), 81530040 (SWG), 81771553 (SWG), 81671436 (XSL) and 81871144 (XSL) from the National Natural Science Foundation of China and an Excellence in Centres of Clinical Medicine grant (2017ZZ01016) from the Science and Technology Commission of Shanghai Municipality. None of the authors have anything to disclose.

Key words: denervation / endometriosis / fibrogenesis / mouse / NK1R / sensory nerve / substance P

Introduction

Endometriosis is a debilitating gynaecologic disease affecting 6–10% of women of reproductive age (Giudice and Kao, 2004). There are three major subtypes of endometriosis, ovarian endometriomas (OE), deep endometriosis (DE) and superficial peritoneal endometriosis (PE), and these subtypes have long been postulated, based on their histology, as three separate disease entities, and, as such, possibly have different pathogenesis and pathophysiology (Nisolle and Donnez, 1997).

OE is the most frequently diagnosed subtype (Jenkins *et al.*, 1986). DE was initially defined as endometriotic lesions infiltrating the peritoneum by >5 mm (Koninckx and Martin, 1992) but is now redefined as adenomyosis externa (Koninckx *et al.*, 2012), and is less prevalent than OE. However, >95% of women with DE complain of severe pain (Koninckx *et al.*, 2012). As such, it is recognized as the most severe clinical form of endometriosis with challenging clinical management (Tosti *et al.*, 2015). While several hormonal and immunological mechanisms have been proposed for DE (Ferrero *et al.*, 2015), the direct evidence in support of these putative mechanisms is lacking.

Our recent study found that both OE and DE lesions exhibited cellular changes consistent with epithelial–mesenchymal transition (EMT), fibroblast-to-myofibroblast transdifferentiation (FMT), smooth muscle metaplasia (SMM) and fibrosis (Liu *et al.*, 2018), as already shown in *in-vitro* and *in-vivo* experimentations (Zhang *et al.*, 2016a, 2016b, 2017). Compared with OE, DE lesions appeared to have undergone more thorough and extensive EMT, FMT and SMM and, consequently, displayed significantly higher fibrotic content but less vascularity (Liu *et al.*, 2018). This raises the question as what other factors are responsible for the development of DE.

More prominently, DE lesions are frequently in proximity with several nerve plexuses: inferior hypogastric, vesical, uterovaginal and rectal plexus. In addition, endometriotic lesions are well-documented to be hyperinnervated (Anaf *et al.*, 2000; Tokushige *et al.*, 2006; Mechsner *et al.*, 2009; Wang *et al.*, 2009), especially in DE (Wang *et al.*, 2009, 2009; Anaf *et al.*, 2011). Apparently, this hyperinnervation is due to the neurogenesis resulting from neutrophins secreted by endometriotic lesions, such as NGF (Barcena de Arellano *et al.*, 2011), NT-3 (Barcena de Arellano *et al.*, 2013) and even thromboxane A2 (TXA_2) (Yan *et al.*, 2017). However, the secreted neutrophins seem to preferentially favour production of sensory neurons at the expense of sympathetic neurons (Ferrero *et al.*, 2010; Arnold *et al.*, 2012), likely because the lesions secrete nerve repellent factors such as semaphorin 3A (Liang *et al.*, 2015).

The striking histological relationship between nerves and the extent of lesional fibrosis (Anaf *et al.*, 2004), especially in DE (Anaf *et al.*, 2000), in contrast to the relatively poorer innervation in OE (McKinnon *et al.*, 2012), raises the possibility that nerves, especially sensory nerves, may facilitate the development and fibrogenesis of endometriosis. We hypothesized that denervation, especially sensory denervation, may decelerate the development and fibrogenesis of endometriosis. In particular, sensory nerve-derived substance P (SP) and its receptor, neurokinin receptor 1 (NK1R), may facilitate the development and fibrogenesis of endometriosis. In this study, we conducted three independent animal experiments to test this hypothesis.

Materials and Methods

Animals

A total of 143 7-week-old virgin female Balb/C mice and 24 immunodeficient nude Balb/C (nu/nu) mice were purchased from the SLAC Experimental Animal Company (Shanghai, China) and used for this study. All mice were maintained under controlled conditions with a 12/12 h light/dark cycle and had access to food and water ad libitum.

All experiments were performed under the guidelines of the US National Research Council's 'Guide for the Care and Use of Laboratory Animals' (2011) and were approved by the Institutional Experimental Animals Review Board of Shanghai Obstetrics and Gynecology Hospital, Fudan University.

Induction of endometriosis

We used an established mouse model of endometriosis by intraperitoneal (i.p.) injection of endometrial fragments (Somigliana *et al.*, 1999) as described in our previous studies (Ding *et al.*, 2015; Long *et al.*, 2016). Briefly, after one week of acclimatization, 7-week-old donor mice were intramuscularly injected with 3 μg/mouse estradiol benzoate (Animal

Medicine Factory, Hangzhou, China) to stimulate the growth of endometrium. One week later they were sacrificed and their uteri were harvested. The uterine tissues were seeded in a Petridish containing warm sterile saline and split longitudinally with a pair of scissors.

Two uterine horns from each mouse were minced with scissors, ensuring that the maximal diameter of the fragment was consistently smaller than 1 mm. The fragments were then injected i.p. to recipient mice. To minimize any individual variation, the endometrial tissue fragments from two donor mice were mixed together and then divided into three or four parts, with each injected i.p. to one mouse each from one of the three or four groups, depending on the experiment design.

Chemical denervation

We used 6-hydroxydopamine (6-OHDA) and resiniferatoxin (RTX) for sympathetic and sensory denervation, respectively, in our mouse studies. 6-OHDA is a sympathomimetic neurotoxin that triggers the release of norepinephrine stores from the sympathetic nerve and selectively destroys the nerve terminals, and is frequently used for sympathetic denervation in rodents (Vaughan *et al.*, 2014). RTX selectively destroys small, unmyelinated mostly C-fibre sensory nerves (Neubert *et al.*, 2003). It is widely used in pain studies to deplete the sensory nerve fibres, leading to thermal analgesia (Almasi *et al.*, 2003; Hsiao *et al.*, 2013; Karai *et al.*, 2004).

To determine the effective doses of 6-OHDA and RTX in adult female Balb/C mice, we tested two doses for each, 6-OHDA (Sigma-Aldrich, St. Louis, MO, USA): 100 mg/kg (Kruszewska *et al.*, 1998) and 200 mg/kg (Gosain *et al.*, 2006); RTX (Sigma-Aldrich): 50 μg/kg (Hsieh *et al.*, 2008) and 200 μg/kg (Kwon *et al.*, 2006), both by i.p. injection. To see how long the putative denervation would produce and last, two mice of each group were sacrificed at 3, 7 and 14 days after serial injections, as outlined below. We used 60 female Balb/C mice in the preliminary experiment, and the results showed that the high dosages were effective in denervation. Therefore, we report the results from high-dosage groups ($n = 30$).

After the preliminary experiment, 14 of 35 mice were randomly selected as donors of uterine fragments, and the remaining 21 mice were randomly divided into three groups of equal sizes: the 6-OHDA group, which received 200 mg/kg i.p. injections of 6-OHDA freshly prepared in sterile saline containing 1% ascorbic acid as an antioxidant (Gosain *et al.*, 2006); the RTX group, which received 200 μg/kg i.p. injections of RTX dissolved in 10% Tween-80 and 10% ethanol in sterile saline (Hsiao *et al.*, 2013); and the control group, which received injections of equal volume of vehicles. To eliminate potential bias caused by different vehicle, the 6-OHDA group was injected with equal volume of RTX vehicle, the RTX group was injected with equal volume of 6-OHDA vehicle, and the control group was injected with the two kinds of vehicles. Designating the day when the endometriosis induction procedure was performed as Day 0, each group received injections every 5 days, starting from Day −3 (i.e. 3 days before induction), and the mice were sacrificed on Day 14 (Supplementary Fig. S1A).

The bodyweight and hotplate latency of all mice were measured and recorded each time before injection (Days −3, 2, 7, 12) and before sacrifice (Day 14) by cervical dislocation. The abdominal cavities were immediately opened up and all lesion tissues were harvested. The total weight of all lesions from each mouse was assessed and then fixed immediately in 4% paraformaldehyde and embedded in paraffin for pathologic examination, histological and immunohistochemical analyses. The endometriotic epithelium and stroma were confirmed by haematoxylin and eosin (H&E) staining.

Hotplate test

The hotplate test was performed with a commercially Hotplate Analgesia Meter (Model BME-480, Institute of Biomedical Engineering, Chinese Academy of Medical Sciences, Tianjin, China) as reported previously (Lu *et al.*, 2010). Since mice are not vocal about their pain severity, and since women with endometriosis as well as rodents with induced endometriosis exhibit central senitization (He *et al.*, 2010; Lu *et al.*, 2010), the hotplate latency can be used as a proxy for the severity of endometriosis-related generalized hyperalgesia (Bannon and Malmberg, 2007). Mice were brought to the testing room and allowed to acclimatize for 10 min before the test. The withdrawal latencies of the hind paws to thermal stimulations were determined in seconds. From the moment when the mouse was placed into the cylinder, the criteria of withdrawal included shaking or licking of its hind paws, or jumping on the hotplate. The latency was calculated as the mean of two sessions separated by a 60-min interval.

Surgical denervation

To further confirm the effect of sensory denervation on lesional development, we also performed surgical denervation. A total of 24 nude mice were randomly divided into three equal-sized groups: the BEFORE group that received surgical denervation 3 days (Day −3) before the heterotransplantation of endometriotic fragments (Day 0), the AFTER group that received surgical denervation 3 days (Day 3) after the transplantation, and the Control group that received a sham surgery at Day −3 without denervation (Supplementary Figure S1B). During the whole experimental procedure, all nude mice were injected with 100 μg/kg estradiol benzoate (Animal Medicine Factory, Hangzhou, China) every 3 days.

For surgical denervation, the nude mice were anaesthetized by i.p. injection of 300 mg/kg chloral hydrate, and the neurectomy was performed as described previously (Shu *et al.*, 2015). Briefly, a midline incision ~2 cm in length at the paravertebral line was made. The skins and subcutaneous tissues were separated, and the T9 to L1 vertebrae were exposed. The nerve roots were exposed unilaterally, and the nerve ~0.5 cm in length was transected distal to the point of trifurcation, followed by wound closure. After surgery, all mice were administrated with penicillin of 40 000 U intramuscularly to prevent infection. After recovery from anesthesia, the mice were pricked with a needle at the wound site, and the lack of response indicated successful denervation.

Human endometriotic tissues were harvested from three cycling patients, aged 31–38 years (mean = 34.7 years), with laparoscopically and histologically diagnosed OE but no hormonal treatment in the last 3 months before surgery. Pieces of lesion tissues were obtained in surgery and immediately transferred into 4°C Dulbecco's modified Eagle's medium/Ham's F-12 medium (DMEM/F-12, Hyclone) supplemented with 100 IU/mL penicillin G, 100 μg/mL streptomycin and 2.5 ug/mL Amphotericin B. Under a laminar-flow hood, the tissues were washed in phosphate-buffered saline to remove red blood cells and debris, and chopped into small pieces of ~1 mm^3 in size (Zamah *et al.*, 1984). The fragments were injected subcutaneously on the denervated regions of the dorsum. All mice received a single injection of 10 pieces of fragments immersed in 200 μL of serum-free DMEM/F–12. Subcutaneous injections were performed using a 1-mL syringe and a 18-gauge needle (Kuligowska, *et al.*, 2005).

Two weeks after the transplantation, all mice were sacrificed. Their bodyweight and hotplate latency were evaluated and recorded before the denervation surgery, the transplantation and sacrifice. By eyeball enucleation, ~700 μL of peripheral blood was drawn from the inner canthus vein of the right eye for baseline measurement of serum soluble P-selectin (sP-sel) levels. Then all lesions on the dorsum were immediately excised, and processed for quantification, and histochemistry and immunohistochemistry (IHC) analysis.

NK1R antagonism

Among the 48 female adult Balb/C mice, 16 of were randomly selected as donors of uterine tissues, and the remaining 32 were recipients that

received uterine tissues. SP and aprepitant, a potent and selective NK1R antagonist, were used to activate and inhibit the NK1R signalling pathway, respectively. The recipient mice were randomly divided into four equal-sized groups, control (CTL), SP, Before-Induction and After-Induction. One day before the induction of endometriosis, mice in CTL, SP and Before-Induction groups were infused with sterile saline, SP (10 μg/kg/day; Sigma, St Louis, MO, USA) (Foldenauer *et al*., 2012) or aprepitant (1 mg/kg/day; Selleck Chemicals, Houston, TX, USA) (Tattersall *et al*., 2000), respectively, via Alzet osmotic pumps (Model 1004, DURECT Corp, Cupertino, CA, USA). Two weeks after induction of endometriosis, the After-induction group was infused with aprepitant via Alzet osmotic pumps (model 1002) in the same dose as the Before-induction group (Supplementary Fig. S1C). The pump ensured consistent and controlled release of contents with a uniform speed. As reported previously (Long *et al*., 2016), we inserted the osmotic pumps on the nape (Supplementary Fig. S2). All mice were sacrificed 4 weeks after the induction of endometriosis. Bodyweight and hotplate latency were evaluated before sacrifice by cervical dislocation. The abdominal cavities were immediately opened up and all lesions were excised and processed for quantification and IHC analysis and the extent of fibrosis was evaluated by Masson trichrome staining.

Immunohistochemistry

Tissue samples were fixed with 10% formalin (w/v) and paraffin embedded. Serial 4 μm sections were obtained from each block, with the first resultant slide being stained for hematoxylin and eosin to confirm pathological diagnosis, and the subsequent slides stained for proliferating cell nuclear antigen (PCNA) (1:50; Abcam, Cambridge, UK), vascular endothelial growth factor (VEGF) (1:50; Abcam), Collagen I (1:200; Abcam), neurokinin 1 receptor (NK1R) (1:50; Santa Cruz) and CD41 (1:200; Abcam) for platelets. Routine deparaffinization and rehydration procedures were performed. For positive controls, mouse brain tissues were used for NK1R, and human OE tissues were used for PCNA, VEGF, α-SMA, collagen I, vimentin, while the human deep endometriosis tissue sample was used for desmin and SM-MHC. For negative controls, we used IgG from rabbit serum instead of the primary antibodies (Supplementary Fig. S3).

For antigen retrieval, the slides were heated at 98°C in a citrate buffer (pH 6.0) for a total of 30 min and cooled to room temperature. The slides were then incubated with the primary antibodies overnight at 4°C. After the slides were rinsed, the horse radish peroxidae-labelled secondary antibody Detection Reagent (Sunpoly-HII; BioSun Technology Co, Ltd, Shanghai, China) was added and incubated at room temperature for 30 min. The bound antibody complexes were stained for 3–5 min or until appropriate for microscopic examination with diaminobenzidine and then counterstained with hematoxylin (30 s) and mounted. Images were obtained with the microscope (Olympus BX53; Olympus, Tokyo, Japan) fitted with a digital camera (Olympus DP73; Olympus). Three to five randomly selected images at ×400 magnification of each sample were taken to get a mean optional density value by Image Pro-Plus 6.0 (version 6.0.0.206; Media Cybernetics, Inc, Bethesda, MD, USA). For PCNA, the percentage of PCNA positive cells stained in brown in nucleus in proportion to the entire field in pixel of the ectopic implants were calculated using Image Pro-Plus 6.0 (Media Cybernetics).

Masson trichrome, Van Gieson and Picro-Sirius red staining

Masson trichrome staining, Van Gieson staining and Picro-Sirius red staining were employed to detect collagen fibres in lesions.

For Masson trichrome staining, tissue sections were deparaffinized in xylene and rehydrated in a graded alcohol series and then were immersed in Bouin solution at 37°C for 2 h. Bouin solution was made with 75 mL of saturated picric acid, 25 mL of 10% formalin (w/v) solution, and 5 mL of acetic acid. Tissue sections were stained using the Masson Trichrome Staining kit (Baso, Wuhan, China) following the manufacturer's instructions. The areas of the collagen fibre layer stained in blue in proportion to the entire field of the ectopic implants were calculated by the Image Pro-Plus 6.0 (Media Cybernetics).

For Van Gieson staining, the tissue sections were heated at 60°C for 45 min, then deparaffinized in xylene and rehydrated in a graded alcohol series. To stain nuclei, sections were dipped into Weigert iron hematoxylin for 10 min, rinsed with tap water, then dipped into 0.1% HCl–ethanol (v/v) for 10 s, and washed with tap water. The sections were then counterstained with Van Gieson solution (Goodbio, Wuhan, China) for 5 min before rinsing with tap water, as our previous method (Liu *et al*., 2016). The areas of the collagen fibre layer stained in red relative to the entire portion of the ectopic implants were calculated by the Image Pro-Plus 6.0 and used as the extent of fibrosis in the lesion.

For Picro-Sirius red staining, tissue sections were heated in an oven at 60°C for 45 min, and then deparaffinized in xylene and hydrated using increasing graded ethanol solutions. The tissue slides were placed in a Picro-Sirius red stain solution kit (Goodbio) for 20 min following the manufacturer's instructions, and rinsed with tap water for 1 min, as our previous work (Liu *et al*., 2016). Under the optical microscope, collagen fibres were stained in red while the epithelium, blood vessels and muscle appear yellowish. The areas of the collagen fibre layer stained in red relative to the entire portion of the ectopic implants were calculated by the Image Pro-Plus 6.0 and used as the extent of fibrosis in the lesion.

Immunofluorescence

Sections were heated for antigen retrieval in the citrate buffer (pH 6.0), then they were incubated with 5% goat serum for blocking non-specific binding sites. The slides were then incubated overnight at 4°C with primary antibodies, including rabbit anti-mouse tyrosine hydroxylase (TH) (1:200; Abcam), and rabbit anti-mouse calcitonin gene-related peptide (CGRP) (1:200; Abcam) antibodies. The slides were incubated with 1:500 AlexaFluor 647-conjugated goat anti-rabbit secondary antibody (Cell Signalling Technology) for 1 h at 37°C. Counterstaining of nuclei with DAPI (Beyotime, Shanghai, China) was also performed. Fluorescent slides were examined under a confocal laser scanning microscope (Leica TCS SP5 Confocal Microscope, Solms, Germany) at room temperature and then exported as a TIFF-format digital file. Image-Pro Plus 6.0 was used to process the images (brightness and contrast) and to construct merged images.

Quantification of sP-selectin by ELISA

The collected blood samples were allowed to clot for 2 h at room temperature, then centrifuged for 20 min at 2000 *g* to obtain serum samples. The resultant samples were analysed by the mouse sP-selectin ELISA kit from R&D Systems (Minneapolis, MN, USA) following the manufacturer's instructions.

Statistical analysis

The comparison of distributions of continuous variables between or among two or more groups was made using the Wilcoxon's and Kruskal's test, respectively, and the paired Wilcoxon test was used when the before–after (induction of endometriosis) comparison was made for the same group of subjects. The standard errors for the ratios of group means were calculated by the Delta method. Pearson's correlation coefficient was used to quantify correlation between two variables when at least one was ordinal or both were continuous. Multivariate linear regression analyses were used to determine which factors were associated with lesion weight, hotplate latency or immunostaining levels. *P*-values of less than

0.05 were considered statistically significant. All computations were made with R 3.5.1 (R Core Team, 2018).

Results

6-OHDA and RTX induce specific denervation in mice

To ensure that the chemical denervation exerts its effect on specific nerve fibres, we first examined 6-OHDA-induced denervation on sympathetic nerves and RTX-induced denervation on sensory DRG neurons. We found that, after serial i.p. injection of 6-OHDA (200 mg/kg), the mean fluorescence intensity of TH-positive neurons was progressively decreased, reaching the lowest level on Day 14, which was merely 9.7% of that in the control group (Fig. 1). Similarly, in mice received serial i.p. injection of RTX (200 μg/kg), the mean fluorescence intensity of CGRP+ neurons was reduced progressively, also reaching the lowest level on Day 14, which was only 8.5% of that in the controls (Fig. 1). No mice died from the procedure. Thus, with the dose and injection schedule that we used, 6-OHDA and RTX effectively denervated sympathetic and sensory nerves, respectively, in mice.

The chemical denervation resulted in some noticeable physiological changes in mice. During the first few hours after the administration of 6-OHDA, the mice displayed hunched back, raised fur and reduced motor activity, a sign indicating specific sympathetic denervation. In addition, varying degrees of diarrhoea were observed and lasted throughout the entire experimental period, resulting in progressive weight loss (Fig. 2A), which indicated a desensitized sympathetic nervous system (Mathias *et al.*, 1985). In particular, the growth curve in mice receiving 6-OHDA was significantly flatter than that of control mice, as measured by the AUC of the bodyweight starting at Day −3 ($P = 0.007$), even though there was no difference at the baseline ($P = 0.56$). In contrast, no significant difference in AUC was found between mice receiving RTX and control mice ($P = 0.38$). Mice with RTX-induced neuropathy exhibited mechanical and thermal hypoalgesia, which were reflected respectively by hypoalgesia-induced self-mutilation (dried blood stains in extremities) and longer hotplate latencies (Fig. 2B).

Chemical denervation reduces lesional size and improves hyperalgesia in mice with induced endometriosis

Denervation of sympathetic and sensory nerves reduced the lesion weight by 43.2% (±23.1%) and 68.7% (±20.3%), respectively, as compared with controls ($P = 0.004$ and $P = 0.0006$, respectively; Fig. 2C, Supplementary Fig. S4). In particular, sensory denervation led to significantly greater reduction in lesion weight than sympathetic denervation ($P = 0.038$; Fig. 2C).

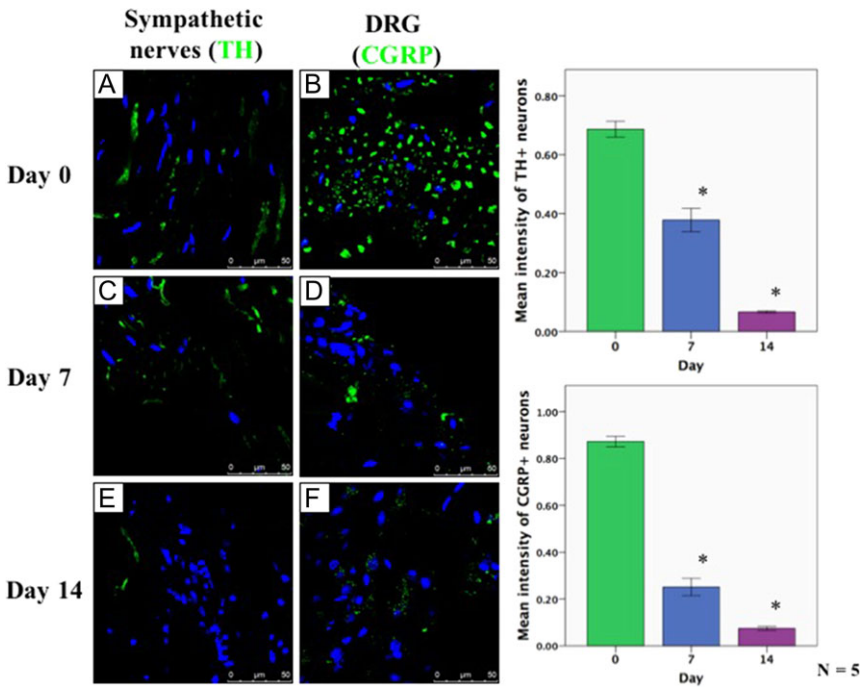

Figure 1 Summary results of chemical denervation. Left panel: Representative photomicrographs of immunofluorescence staining of TH positive sympathetic nerves (**A**, **C** and **E**) and CGRP positive sensory nerves in DRG neurons (**B**, **D** and **F**) that were evaluated at 0, 7 and 14 days after chemical denervation with 200 mg/kg of 6-OHDA (A, C and E) and 200 μg/kg of RTX (B, D and F), respectively. Magnification: ×400. Scale bar = 100 μm. Right panel: Summary of the mean intensity of immunofluorescence staining of TH positive sympathetic neurons and of CGRP positive sensory neurons that were evaluated at 0, 7 and 14 days after chemical denervation by 6-OHDA and of RTX, respectively. $N = 5$ for each chemical and each time point. Data are presented as mean ± SD. *$P < 0.05$.

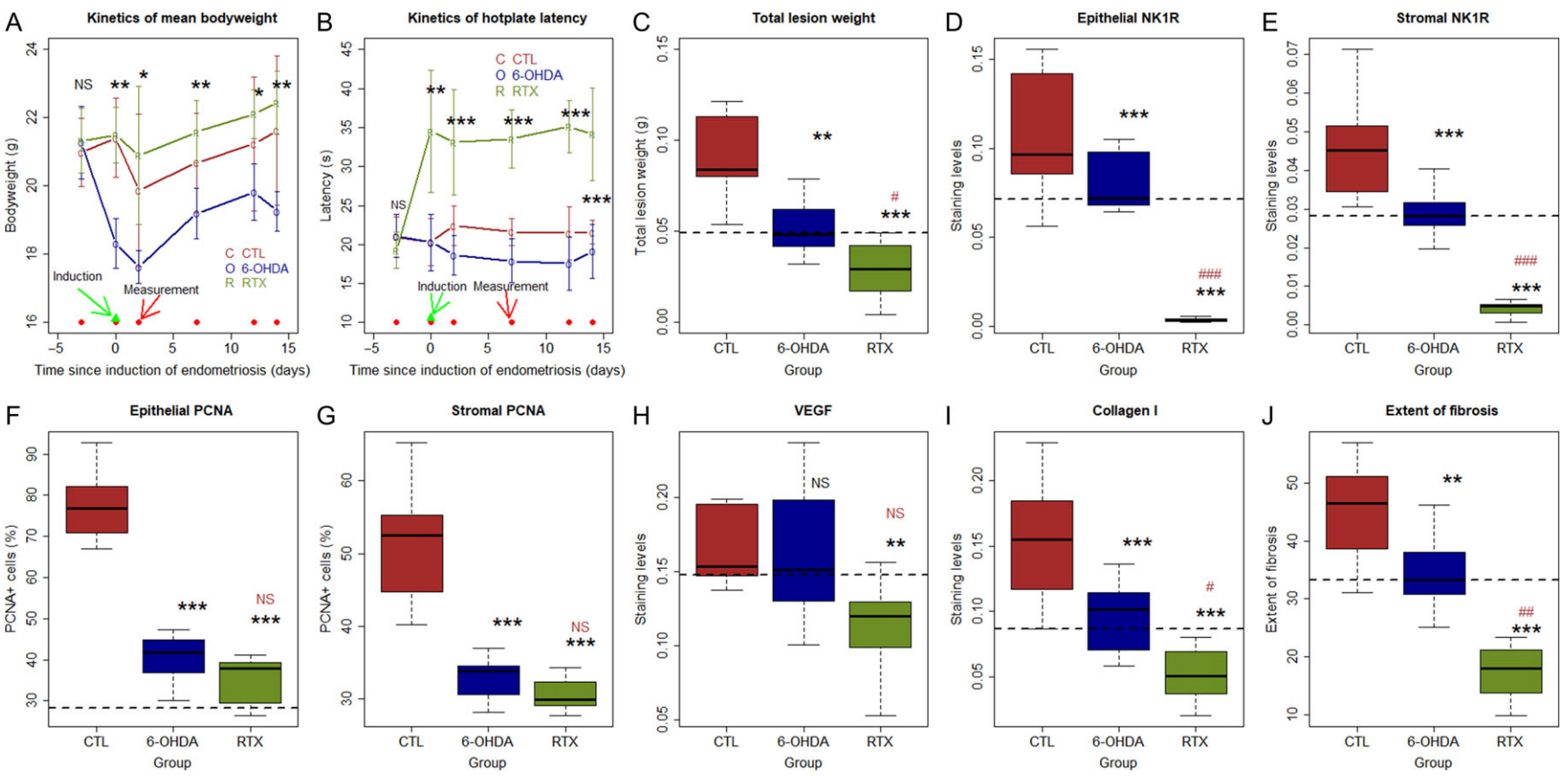

Figure 2 Summary results of Experiment 1. The dynamic changes of mean bodyweight (**A**) and hotplate latency (**B**) in mice treated with vehicle, 6-OHDA or RTX. The data are shown in means and standard deviations. Boxplot of lesion weight (**C**), staining of NK1R in the epithelial (**D**) and the stromal components (**E**), the percentage of PCNA-positive cells in the epithelial (**F**) and stromal components (**G**), staining of VEGF (**H**), and collagen I (**I**) and the extent of fibrosis (**J**) among different groups. Symbols for the statistical significance levels: * or #: $P < 0.05$, ** or ##: $P < 0.01$; *** or ###: $P < 0.001$; NS, not statistically significant, i.e. $P > 0.05$, all by Wilcoxon's rank test (Kruskal's test in (A) and (B)). The symbols for significance levels are, in black, for the designated group versus the control group, or, in red, versus the 6-OHDA group. At all time points $n = 7$ for each group.

While all mice had similar hotplate latency before the chemical denervation ($P = 0.29$; Fig. 2B), sensory denervation resulted in significantly increased latency in mice as compared with controls, starting from the day of endometriosis induction (all P-values <0.012; Fig. 2B). In contrast, sympathetic denervation yielded significantly reduced latency just 2 days after the induction (all P-values ≤0.026, but $P = 0.055$ on Day 14; Fig. 2B), indicating that sympathetic denervation did not improve endometriosis-associated hyperalgesia as sensory denervation did, and may in fact have exacerbated it.

Chemical denervation reduces lesional expression of markers for proliferation, angiogenesis and fibrosis

We also performed an IHC analysis of NK1R, PCNA, VEGF and collagen I, along with Masson trichrome staining, in lesion samples. We summarized the locations and cellular components of the staining of different IHC markers in Table I. Figure 3 shows the representative IHC results, and Fig. 2D–J summarizes the results.

Of note, NK1R staining was found in both epithelial and stromal components of ectopic endometrium, especially in its epithelial component, but both sensory and sympathetic denervation significantly reduced the staining levels (all P-values <0.001 by regression, both $R^2 = 0.95$; Fig. 2). In particular, sensory-denervated mice had significantly lower NK1R staining levels than those received sympathetic denervation (both P-values = 0.0006; Fig. 2D and E), likely resulting from reduced secretion of SP by sensory nerves due to reduced sensory nerve fibres.

Through linear regression analysis with adjustment for bodyweight, we found that both sympathetic and sensory denervation resulted in a lower percentage of PCNA+ cells (in both epithelial and stromal components), lower immunoreactivity against collagen I and a lower extent of fibrosis in ectopic endometrium as compared with control mice (all P-values <0.0022, all $R^2 \geq 0.75$; Fig. 2F, G, I, J). Sensory, but not sympathetic, denervation, also significantly reduced the VEGF immunostaining levels as compared with control mice (all $P = 0.0052$, $R^2 = 0.34$; Fig. 2H). In particular, sensory denervation resulted in significantly lower immunostaining levels of NK1R and collagen I as well as significantly lower extent of fibrosis in lesions than did sympathetic denervation (all P-values <0.018; Fig. 2D, E, I, J).

The NK1R staining levels in both epithelial and stromal components were found to correlate positively with the lesion weight (all $r \geq 0.89$, all $P < 8.7 \times 10^{-8}$), PCNA (all $r \geq 0.77$, all $P < 4.7 \times 10^{-5}$), VEGF (all $r \geq 0.73$, all $P < 1.7 \times 10^{-4}$). In endometriotic stroma, the NK1R staining levels correlated positively with collagen I staining ($r = 0.94$, $P = 5.0 \times 10^{-10}$), and particularly the extent of fibrosis ($r = 0.97$, $P = 6.8 \times 10^{-13}$) but negatively with the hotplate latency ($r = -0.90$, $P = 2.4 \times 10^{-8}$), suggesting that SP-NK1R signalling pathway plays an important role in the development of endometriosis.

Surgical denervation decelerates the development of endometriosis

RTX is known to be a potent NF-κB inhibitor (Singh *et al.*, 1996), yet the role of NF-κB in endometriosis is well-documented (Guo, 2007; Gonzalez-Ramos *et al.*, 2010). The retarded lesional development in RTX-treated group may thus be attributable, perhaps in no small amount, to suppressed NF-κB activity. To further determine the effect of sensory denervation on lesional development, we performed a denervation surgery by severing the spinal nerves. We transected sensory nerves ~0.5 cm in distance distal to the point of trifurcation clinging to dorsal root just outside the spinal cord (Shu *et al.*, 2015). Consistent with the results from the chemical denervation experiment, denervation before and after the induction of endometriosis reduced lesion weight by an average of 64.4% (±47.3%) and 60.5% (±20.9%), respectively, as compared with controls (both P-values≤0.015; Fig. 4A, Supplementary Fig. S5). While denervation before induction resulted in greater reduction in lesion weight than the after induction, the difference did not reach statistical significance level ($P = 0.34$; Fig. 4A).

Consistent with the decelerated lesion growth resulting from surgical denervation, there was a significant difference in hotplate latency among the three groups at the end of the experiment ($P = 0.002$) even though no such difference was found at the baseline ($P = 0.58$) or 3 days before induction ($P = 0.40$; Fig. 4B). In particular, mice in the before- and after-induction groups both had significantly longer latency than mice without denervation (both P-values ≤0.005; Fig. 4B).

We also performed an IHC analysis of NK1R staining and, for quantification of the extent of fibrosis, Masson trichrome, Van Gieson and Picro-Sirius red stainings. Consistent with the findings in chemical denervation experiment, surgical denervation before and after the induction of endometriosis significantly decreased the NK1R staining levels in both epithelial and stromal components (P's = 0.0002 and P's = 0.0009, respectively; Figs 4C, D and 5). In addition, surgical denervation both before and after the induction of endometriosis

Table I Cellular component, location and staining intensity of different immunohistochemistry markers.

Marker name	Found mostly in which cell type	Location of the staining	Staining intensity	Scoring in which component
PCNA	Both in endometriotic glandular epithelial and stromal cells (mainly in epithelial cells)	Cell nucleus	Strong; decreased after both sensory and sympathetic denervation	Glandular epithelial cells
VEGF	Glandular epithelial cells	Cytoplasm	Medium; decreased after sensory denervation	Glandular epithelial cells
Collagen I	Endometriotic stromal cells	Extracellular matrix of the stromal tissues	Medium–strong; decreased after sensory denervation	Stromal component of the ectopic lesions
NK1R	Glandular epithelial cells	Cytoplasm	Medium; decreased after sensory denervation	Glandular epithelial cells

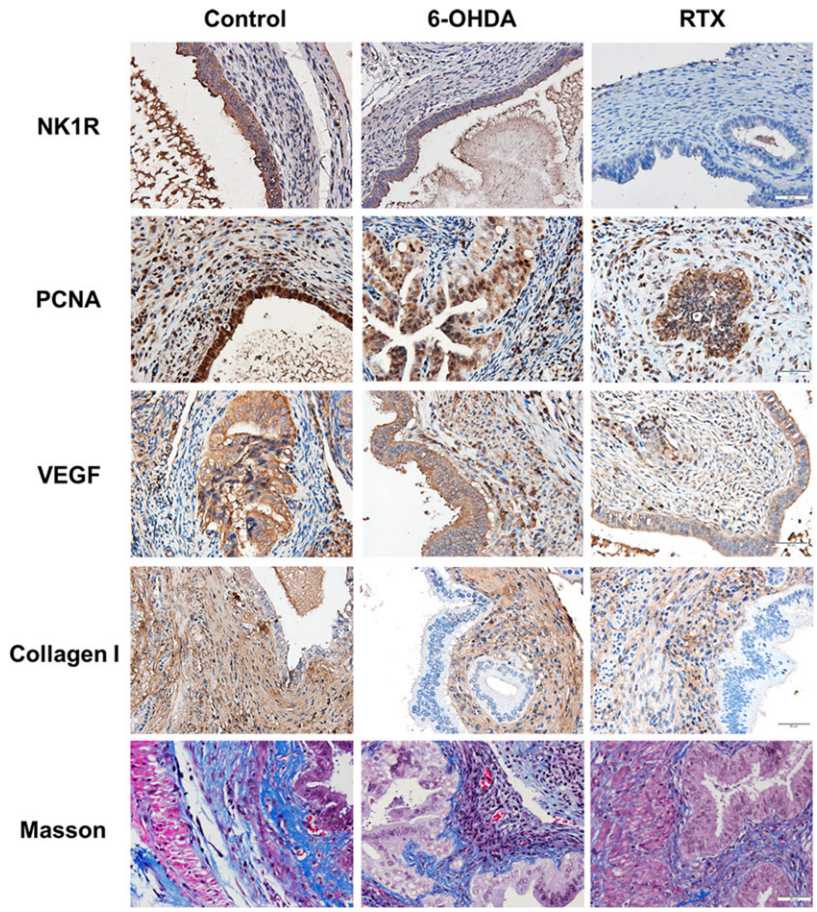

Figure 3 Immunohistochemistry and histochemistry analyses for Experiment 1. Representative immunostaining and Masson trichrome staining results in ectopic lesions in mice treated with 6-OHDA and RTX. Scale bar = 50 μm.

resulted in significantly reduced platelet aggregation in lesions (P = 0.038 and P = 0.00016, respectively; Figs 4E and 5). Consistently, surgical denervation also significantly reduced the serum sP-sel levels (P = 0.0499 and P = 0.00016, respectively; Fig. 4F), which were correlated with the extent of lesional platelet aggregation (r = 0.94, P = 9.8 × 10^{-12}). Lesional NK1R staining levels correlated with the extent of platelet aggregation (all $r \geqq 0.75$, all $P \leq 2.6\times10^{-5}$).

The three histologic staining methods yielded nearly identical results, with the correlation coefficient between any two methods being 0.97 or greater ($P < 3.3\times10^{-16}$). By all staining methods, denervation both before and after the induction significantly reduced the extent of lesional fibrosis as compared with controls (all P-values <0.00016; Figs 4G and 5, and Supplementary Fig. S6A, B). Under the optical microscope, the Picro-Sirius red staining sections of control group showed mostly bright red in the stroma, indicative of collagen fibres, while the lesions taken from surgically denervated mice appeared mainly yellow in endometriotic epithelial and stromal compartments as well as the vascular epithelium. Van-Gieson staining appeared mostly red, indicating collagen fibres in control group, while the lesions of both before- and after-induction groups showed mostly epithelium and muscle fibres (mostly epithelium) stained yellowish (Fig. 5). Importantly, the extent of lesional fibrosis correlated negatively with the hotplate latency (all $r \leq -0.64$, all $P \leq 7.6 \times 10^{-4}$; Fig. 4H).

Consistently, the NK1R staining levels in endometriotic lesions correlated positively with the lesion weight (all $r \geqq 0.83$, all $P \leq = 1.1 \times 10^{-6}$ (with one apparent outlier removed); Supplementary Fig. S6C,D) and the extent of fibrosis (all $r \geqq 0.93$, all $P \leq 2.9 \times 10^{-11}$; Supplementary Fig. S6E,F) but negatively with the hotplate latency (all $r \leq -0.67$, all $P \leq 3.5 \times 10^{-4}$; Supplementary Fig. S6G,H). Lesion weight also correlated with the extent of fibrosis (all $r \geqq 0.76$, $P = 1.6 \times 10^{-5}$ for all three staining methods). Combined with the chemical denervation data, it can be concluded that sensory denervation decelerated the lesional development.

NK1R activation accelerates, while NK1R antagonism decelerates, lesional fibrogenesis

Sensory nerves secrete numerous neuropeptides. Among them, SP is the most prominent one. The endogenous receptor for SP is NK1R (Gerard *et al.*, 1991). Given the above findings that sensory denervation

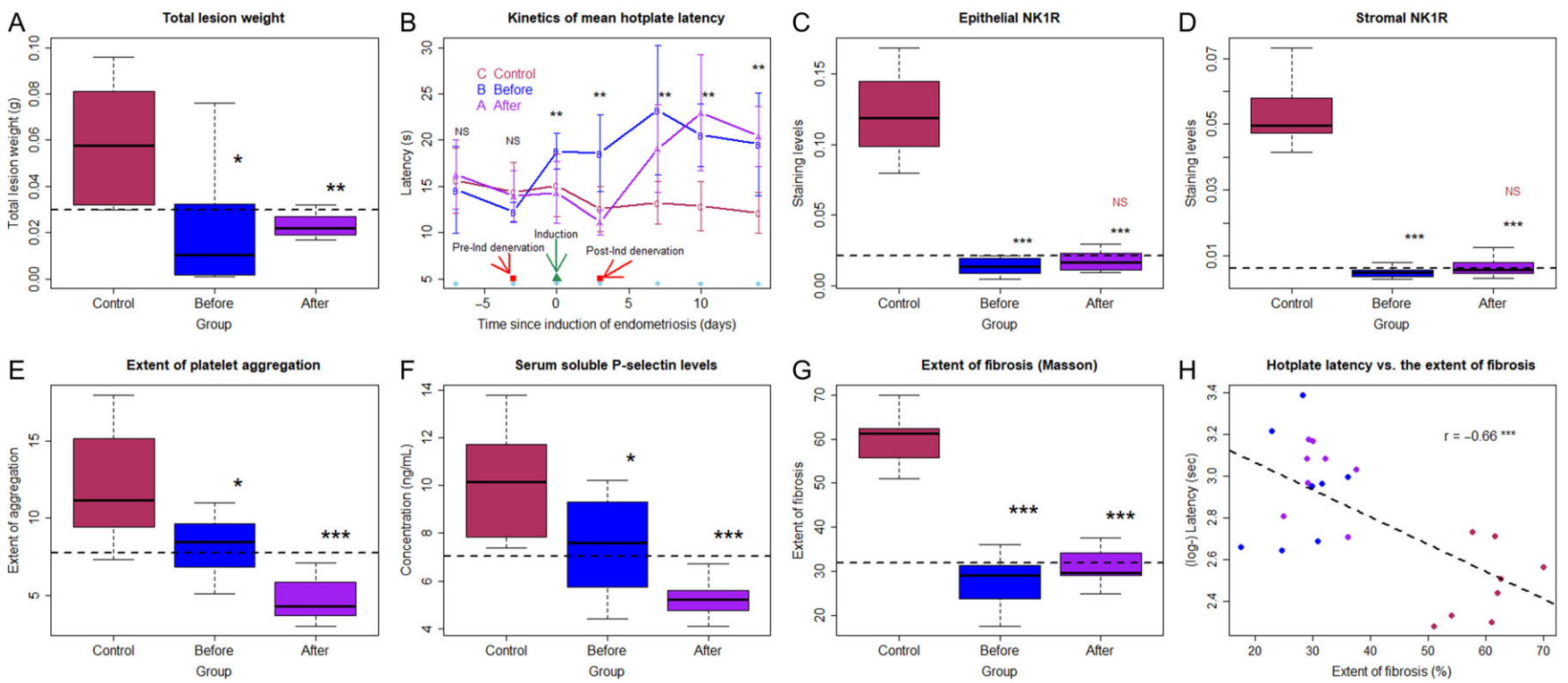

Figure 4 Summary results of Experiment 2. (**A**) Boxplot of lesion weight among different groups of mice. (**B**) The dynamic changes of the mean hotplate latency in different groups. The data are shown in means and standard deviations. The dots in sky blue represent the time when the hotplate test was administrated. The statistical significance in difference in latency at the designated time points among the three groups was shown. Boxplot of lesional NK1R staining in the epithelial (**C**) and the stromal components (**D**), the extent of platelet aggregation (**E**), serum soluble P-selectin levels (**F**) and the extent of lesional fibrosis (**G**) in different groups. (**H**) Scatter plot showing the relationship between hotplate latency and the extent of lesional fibrosis. Pearson's correlation coefficient is shown, followed by its level of statistical significance. The dashed line represents the regression line. Except (B) and (H), the symbols in black and maroon for statistical significance levels are for the designated group versus the Control and the Before group, respectively. Symbols for the statistical significance levels: *$P < 0.05$, **$P < 0.01$, ***$P < 0.001$ (by Wilcoxon rank test or Kruskal test). NS, statistically not significant, i.e. $P > 0.05$. $n = 8$ at all time points for each group.

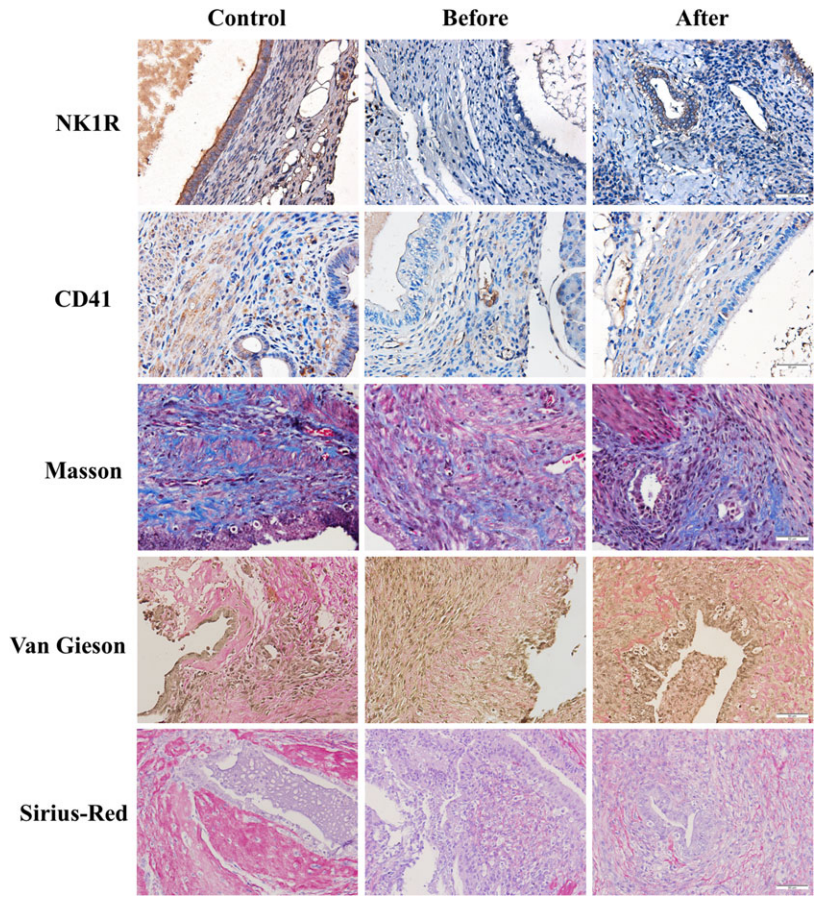

Figure 5 Immunohistochemistry and histochemistry analyses for Experiment 2. Representative results of immunohistochemistry analysis and Masson, Van Gieson and Picro-Sirius red staining of endometriotic lesions in different groups of mice. Scale bar = 50 μm.

significantly decelerates the development and fibrogenesis of endometriosis, we wondered as whether SP infusion and NK1R antagonism have any effect on lesional development.

We found that, compared with controls, mice that received SP infusion had significantly heavier/larger lesions ($P = 0.021$), but NK1R antagonism, either instituted before or after the induction of endometriosis, significantly reduced the lesion weight (both P-values ≤ 0.002; Fig. 6A, Supplementary Fig. S7). On average, the lesions in the SP group was 53.1% (±31.8%) heavier than that of control group, while NK1R antagonism before and after induction reduced the lesion weight by 94.1% (±8.1%) and 54.2% (±22.5%), respectively (Fig. 6A). The lesion weight in the pre-induction group was significantly lower than that of the post-induction group ($P = 0.0009$), indicating that preemptive administration of NK1R inhibitor could retard the initial growth of endometriotic lesions.

Consistently, the SP group had significantly shorter, but both before-induction and after-induction groups had significantly longer, hotplate latency than that of control group (all P-values ≤ 0.0016), even though no such difference was found at the baseline ($P = 0.81$; Fig. 6B). The before-induction group had longer latency than that of the after-induction group, but the difference was only marginally significant ($P = 0.065$).

We also carried out IHC and histological analyses of markers of EMT, FMT, SMM and the extent of fibrosis in endometriotic lesions (Fig. 7). As expected, both before and after groups had nearly absent lesional NK1R expression, significantly lower than that of the control group (all $P \leq 0.008$ and all $P \leq 0.0009$, respectively), while the SP group had significantly higher NK1R expression than that of control group (all $P \leq 0.0011$; Fig. 6C and D). With the only exception of VEGF, the SP group had significantly higher expression of all markers (and for PCNA and α-SMA, both epithelial and stromal components), and lower expression of E-cadherin, than that of controls (all P-values < 0.038). In contrast, both before- and after-induction groups had significantly lower expression of all markers, and higher expression of E-cadherin, than that of control group (all P-values < 0.05; Fig. 8A–I). In particular, the SP group had significantly higher, while both before- and after-induction groups had significantly lower extent of fibrosis than that of control group (all P-values $\leq 3.6 \times 10^{-5}$; $R^2 = 0.89$; Fig. 8J). On average, the fibrotic content in the SP group increased by 92.2% while before- and after-induction groups reduced the content by 71.8 and 50.7%, respectively, as compared with that of control group (Fig. 8J).

Importantly, stromal NK1R staining levels in endometriotic lesions correlated positively with the extent of lesional fibrosis but negatively with the hotplate latency ($r = 0.97$, $P < 2.2 \times 10^{-16}$, and $r = -0.92$,

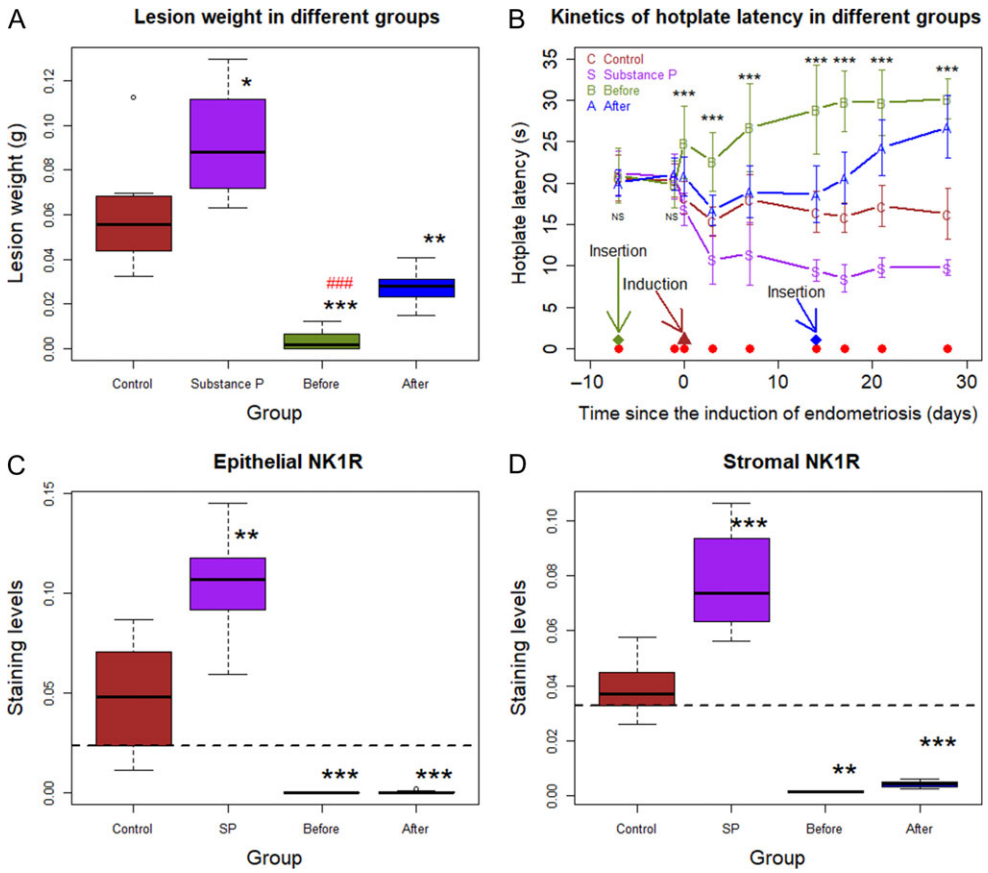

Figure 6 Summary results of Experiment 3. (**A**) Boxplot of lesion weight among different treatment groups. (**B**) The dynamic changes of mean hotplate latency in mice infused with vehicle (Control), substance P (SP), and aprepitant 7 days before (Before) and 14 days after (After) the induction of endometriosis. The data are shown in means and standard deviations. Boxplot of lesional NK1R staining in the epithelial component (**C**) and the stromal component (**D**). The dashed line represents the median value from all three groups. In (A), the symbols for statistical significance levels are for the designated group versus the control group, in black, or versus the After group, in red. In (B), the symbols for statistical significance refer to the comparison among the four groups. In addition,'Insertion' indicates the insertion of the Azlet osmotic pumps, while 'Induction' designates the induction of endometriosis. Symbols for the statistical significance levels (by Wilcoxon rank test, but Kruskal's test in (B)): *$P < 0.05$; **$P < 0.01$; *** or ###: $P < 0.001$; NS: Statistically not significant, i.e. $P > 0.05$. $n = 8$ for each group at all time points. The red dots in (B) represent the time when the hotplate test was administrated.

$P = 2.6 \times 10^{-12}$; Fig. 8K, L, and Supplementary Fig. S8A, B for epithelial staining). They also correlated with markers of EMT, FMT, SMM and the extent of fibrosis (all $r \geq 0.87$ or ≤ -0.89, all $P < 1.7 \times 10^{-9}$; Supplementary Fig. S8C–J). Taken together, these data suggest that SP-NK1R signalling impacts on the all processes of lesional development.

The extent of lesional fibrosis was found to be correlated positively with lesion weight ($r = 0.96$, $P = 2.5 \times 10^{-16}$) but negative with the hotplate latency ($r = -0.87$, $P = 1.5 \times 10^{-9}$; Supplementary Fig. S8K, L).

Discussion

Through three independent yet complementary experimentations, we have shown in this study that denervation, especially sensory denervation, decelerates the development and fibrogenesis of endometriosis. In particular, sensory denervation suppresses NK1R expression in endometriotic lesions, very likely through the reduction in SP release, resulting in greater retardation in lesional progression. In all three experiments, lesional NK1R expression levels correlate positively with the lesion weight and the extent of fibrosis, likely through its promotional effect on EMT, FMT and SMM during the progression of endometriosis (Zhang *et al.*, 2016a).

Nerves are a notable feature of the lesional microenvironment, especially in DE (Anaf *et al.*, 2002, 2011; Wang *et al.*, 2009). Yet aside from their role in pain transduction, their role in lesional development has seemingly received scant, if any, attention, and how they exert their influence on lesional development has been completely unclear. This study demonstrates that sensory nerves may play critical roles in lesional development, likely through the activation of the SP/NK1R signalling pathway. In essence, it demonstrates that sensory nerves are yet another unindicted culprit in the development of endometriosis.

This study has several strengths. First, we employed three independent, yet complementary, experimentations to demonstrate that sensory denervation decelerates the development of endometriosis, and

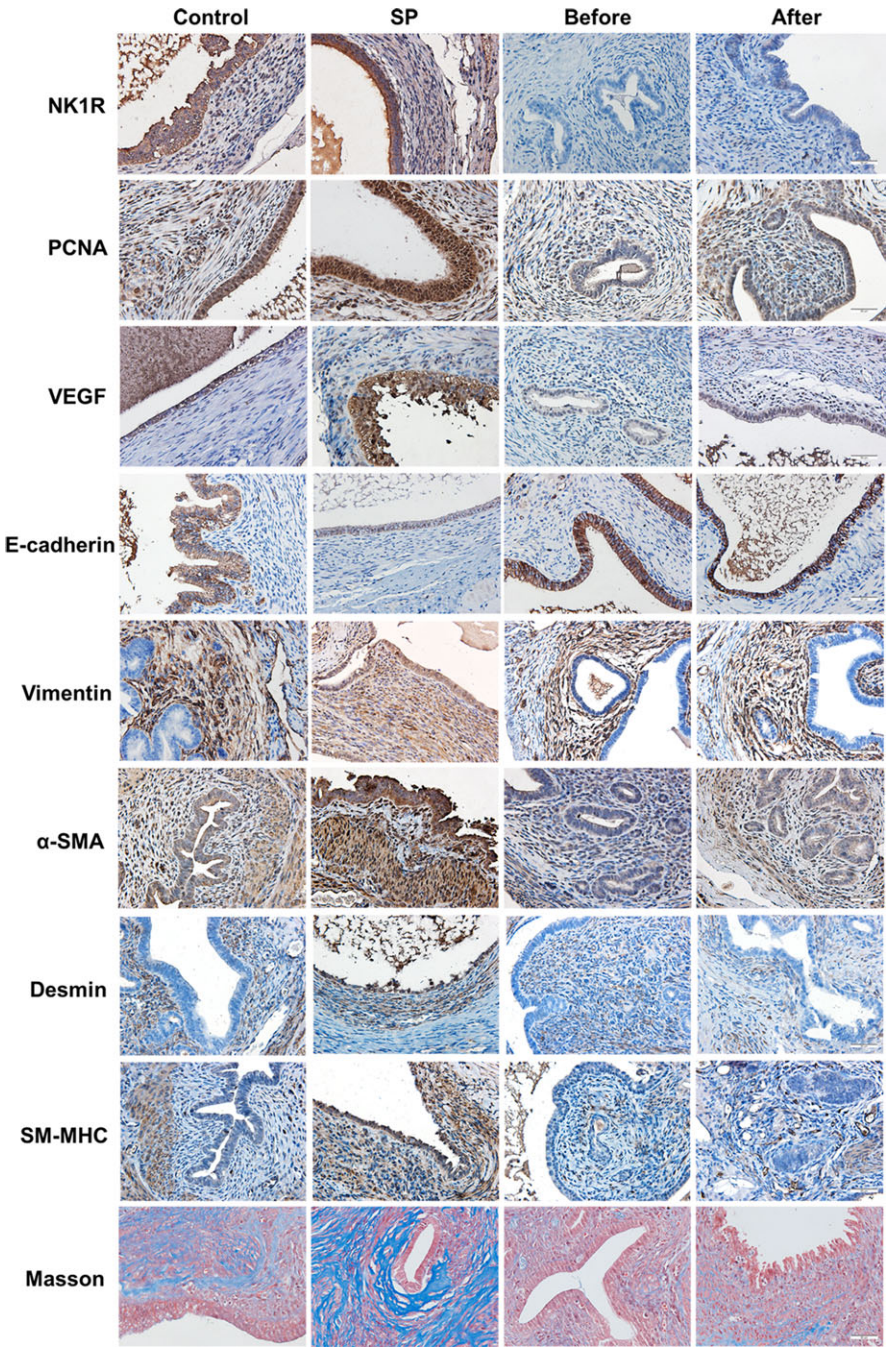

Figure 7 Immunohistochemistry and histochemistry analyses for Experiment 3. Representative results of immunostaining and Masson staining in endometriotic lesions in different groups of mice. Scale bar = 50 μm.

showed that SP-induced NK1R activation facilitates, while NK1R antagonism decelerates, the development of endometriosis. Second, we specifically evaluated markers of EMT, FMT, SMM and the extent of fibrosis in lesions in the experiments that employed both NK1R activation and antagonism, and correlated NK1R staining with lesion weight as well as markers of EMT, FMT, SMM and fibrosis. In this way, we provide evidence to support the roles of SP/NK1R signalling in EMT, FMT, SMM and fibrogenesis.

Of course, our study also has limitations. The most conspicuous one is that our study is limited by the use of histologic and immunohistochemistry analyses only and lacks molecular data. In addition, we did not evaluate the role of other neuropeptides such as CGRP and their receptors since sensory nerves also secrete neuropeptides other than SP.

In general, our findings are consistent with the documented roles of SP/CGRP and their receptors in wound healing and fibrogenesis. SP accelerates the normal acute and chronic wound healing processes

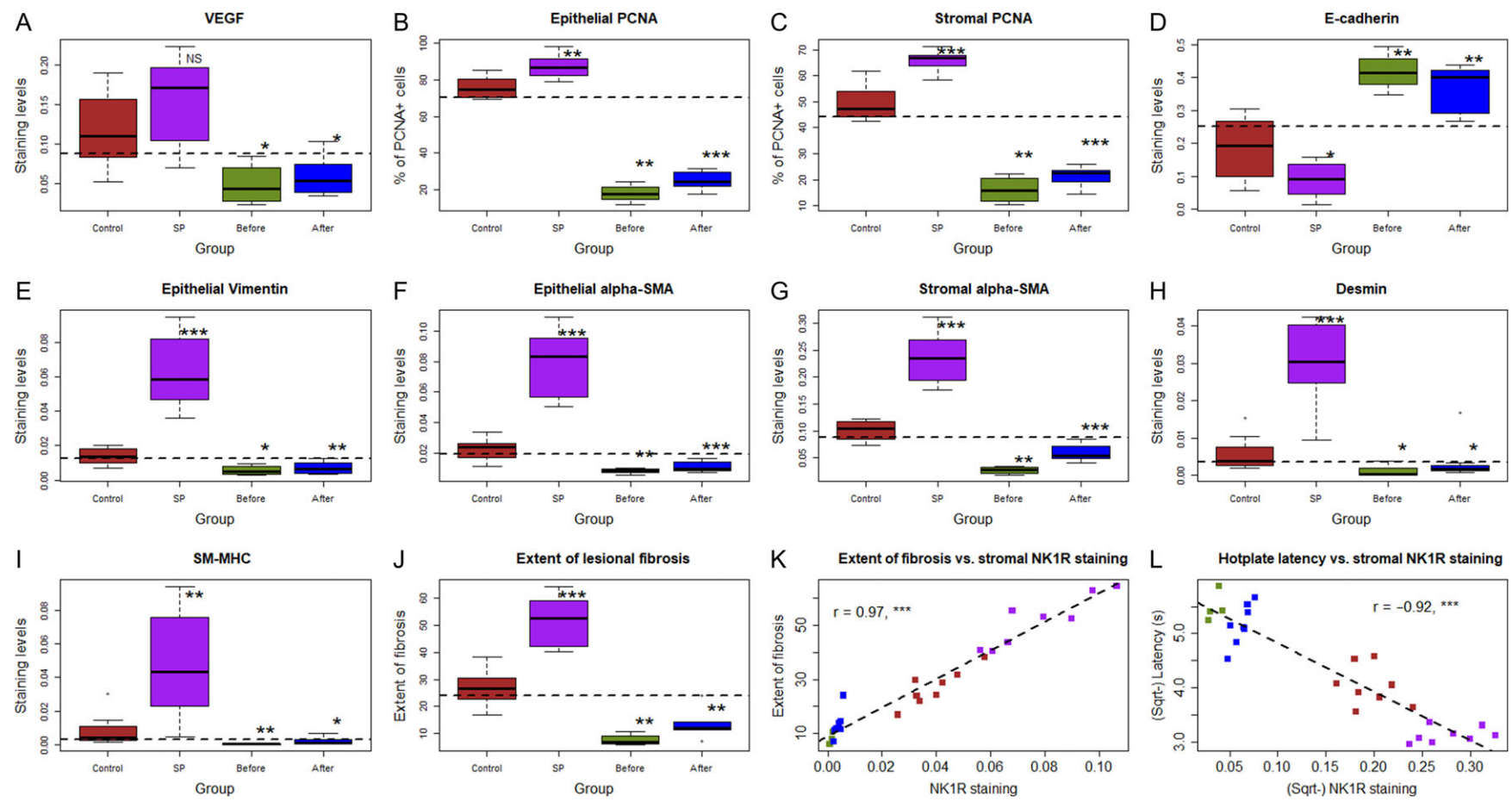

Figure 8 Summary of histochemistry and immunohistochemistry analyses by boxplots. (**A**) VEGF, (**B**) Percentage of PCNA-positive cells in the epithelial (B) and the stromal components (**C**), (**D**) E-cadherin staining, (**E**) vimentin staining in the epithelial component,α-SMA staining in the epithelial (**F**) and stromal components (**G**), and staining levels of desmin (**H**) and SH-MHC (**I**), as well as the extent of lesional fibrosis (**J**) in endometriotic lesions. The dashed line represents the median value from all four groups. All comparisons were made in reference to the Control group, and Wilcoxon's rank test was used. The scatter plot showing the relationship between stromal NK1R staining levels and the extent of lesional fibrosis (**K**) and hotplate latency (**L**). The number shown is the correlation coefficient, followed by its statistical significance level. The dashed line represents the regression line. Symbols for the statistical significance levels: *$P < 0.05$, **$P < 0.01$, ***$P < 0.001$; NS, statistically not significant, i.e. $P > 0.05$.

(Yang *et al.*, 2014; Kant *et al.*, 2015; Leal *et al.*, 2015), while sensory denervation impairs cutaneous wound healing through increased apoptosis and reduced proliferation (Engin *et al.*, 1996; Smith and Liu, 2002). Alternatively, denervation impairs wound healing possibly through reducing the infiltration of inflammatory immune cells in the early stage of healing (Richards *et al.*, 1999; Xiao *et al.*, 2015) which may be a prerequisite for later fibrogenesis. Indeed, renal denervation is reported to attenuate multi-organ fibrosis in rats with induced cardiomyopathy (Liu *et al.*, 2015; Wang *et al.*, 2016) and also to reduce interstitial myocardial fibrosis in patients with resistant hypertension (Doltra *et al.*, 2014).

SP is often used as a marker for sensory nerves in or around endometriotic lesions (Tokushige *et al.*, 2006; Mechsner *et al.*, 2007). Our results that NK1R promotes the development of endometriosis is consistent with the report that NK1R is expressed in endometriotic lesions, especially in peritoneal lesions (McKinnon *et al.*, 2013). SP enhances, while NK1R antagonism reduces, endometrial stromal cell viability, and treatment of endometrial cells with TNFα induces NK1R expression (McKinnon *et al.*, 2013). Conversely, increased nerve fibre density in and around endometriotic lesions (Anaf *et al.*, 2000; Berkley *et al.*, 2004; Tokushige *et al.*, 2006; Mechsner *et al.*, 2007, 2009; Wang *et al.*, 2009) may result in elevated SP concentration within lesions. Alternatively, the elevated IL-1β levels in lesions (Bergqvist *et al.*, 2000) may activate receptors localized on sensory nerve endings, resulting in increased release of SP (Eliav *et al.*, 2009).

Aside from the promotion of lesional platelet aggregation, the SP-NK1R signalling could facilitate the fibrogenesis of endometriosis through many other ways. First, NK1R activates Ca^{2+}, ERK1/2, NF-κB and PKCδ, and stimulates IL-8 gene expression (Lai *et al.*, 2008), which are reported to be involved in fibrogenesis (Luedde and Schwabe, 2011; Chichger *et al.*, 2015; Liu *et al.*, 2017).Second, NK1R activation at the plasma membrane initiates G protein-mediated signalling events (Steinhoff *et al.*, 2014; Garcia-Recio and Gascón, 2015), potentially promoting lesional progression (Perez *et al.*, 2002). Third, SP-NK1R may lead to the activation of phospholipase A2 (PLA_2), formation of arachidonic acid, and generation of prostaglandins, leukotrienes, and TXA_2, through induction of COX-2 expression through JAK-STAT (Koon *et al.*, 2006). PLA_2, leukotrienes and TXA_2 have reported to be implicated in different fibrotic diseases (Nanji *et al.*, 2013; Lei *et al.*, 2015; Kanai, *et al.*, 2016; Lu *et al.*, 2017). Finally, SP may reduce tissue plasminogen activator (tPA) while induce plasminogen activator inhibitor 1 (PAI-1), resulting in decreased fibrinolysis as in postoperative adhesion formation (Esposito *et al.*, 2013; Cassidy *et al.*, 2014) and thus exacerbating lesional fibrosis.

The reduced platelet aggregation in endometriotic lesions that we found in the surgical denervation experiment is consistent with the report that SP stimulates platelet aggregation (Graham *et al.*, 2004). The additional positive feedback regulation of platelet aggregation (Gibbins, 2009) suggests that NK1R may be another anti-platelet target (Jones and Gibbins, 2008).

SP-induced NK1R activation can induce tissue factor (TF) expression and secretion in monocytes (Khan *et al.*, 2012; Yamaguchi *et al.*, 2016). Given the pivotal role of TF in coagulation, SP apparently also plays a role in coagulation. In fact, just like collagen, SP can directly activate platelets (Graham *et al.*, 2004), and SP-NK1R signalling is necessary for thrombus formation (Jones *et al.*, 2008). Thus, SP-NK1R signalling may also promote platelet aggregation in endometriotic lesions. Platelets themselves also release SP (Page *et al.*, 2003; Graham *et al.*, 2004), and the TXA_2 released by activated platelets has been shown to induce neurite outgrowth, resulting in hyperinnervation in lesions (Yan *et al.*, 2017). The increased nerve fibre density, in turn, would also lead to increased concentration of SP in endometriosis, further inducing platelet activation and aggregation. Moreover, SP is reported to induce M2 macrophage activation (Jiang *et al.*, 2012; Lim *et al.*, 2017), but M2 macrophages are known to participate in tissue repair (Lim *et al.*, 2017) and are involved in promoting lesion growth and fibrogenesis in endometriosis (Duan *et al.*, 2018). Further research is required to delineate the roles of SP/NK1R signalling pathway in facilitating lesional development.

In summary, we have shown in this study that sensory denervation decelerates the development and fibrogenesis of endometriosis, likely through the suppression of the SP/NK1R signalling pathway in endometriotic lesions, which may actively participate in inducing EMT, FMT, SMM and fibrogenesis. Our study demonstrates that sensory nerves are likely an active accessory to endometriotic cells to accelerate lesional development in addition to their traditionally perceived roles as pain transducers. Sensory nerves are yet another unindicted culprit in the development of endometriosis, and, as such, NK1R may be an admissible drug target for treating endometriosis.

Supplementary data

Supplementary data are available at *Human Reproduction* online.

Authors' roles

S.W.G. conceived and designed the study, performed data analysis and data interpretation, and drafted the article. X.S.L. and D.Y. performed all the experiments and carried out data analysis. All authors participated in the writing and approved the final version of the article.

Funding

National Natural Science Foundation of China (81471434, 81530040 and 81771553 to S.W.G.; 81671436 and 81871144 to X.S.L.) and an Excellence in Centres of Clinical Medicine grant (2017ZZ01016) from the Science and Technology Commission of Shanghai Municipality.

Conflict of interest

All authors state that they have nothing to declare.

References

Almasi R, Petho G, Bolcskei K, Szolcsanyi J. Effect of resiniferatoxin on the noxious heat threshold temperature in the rat: a novel heat allodynia model sensitive to analgesics. *Br J Pharmacol* 2003;**139**:49–58.

Anaf V, El Nakadi I, De Moor V, Chapron C, Pistofidis G, Noel JC. Increased nerve density in deep infiltrating endometriotic nodules. *Gynecol Obstet Invest* 2011;**71**:112–117.

Anaf V, El Nakadi I, Simon P, Van de Stadt J, Fayt I, Simonart T, Noel JC. Preferential infiltration of large bowel endometriosis along the nerves of the colon. *Hum Reprod* 2004;**19**:996–1002.

Anaf V, Simon P, El Nakadi I, Fayt I, Buxant F, Simonart T, Peny MO, Noel JC. Relationship between endometriotic foci and nerves in rectovaginal endometriotic nodules. *Hum Reprod* 2000;**15**:1744–1750.

Anaf V, Simon P, El Nakadi I, Fayt I, Simonart T, Buxant F, Noel JC. Hyperalgesia, nerve infiltration and nerve growth factor expression in deep adenomyotic nodules, peritoneal and ovarian endometriosis. *Hum Reprod* 2002;**17**:1895–1900.

Arnold J, Barcena de Arellano ML, Ruster C, Vercellino GF, Chiantera V, Schneider A, Mechsner S. Imbalance between sympathetic and sensory innervation in peritoneal endometriosis. *Brain Behav Immun* 2012;**26**:132–141.

Bannon AW, Malmberg AB. Models of nociception: hot-plate, tail-flick, and formalin tests in rodents. *Curr Protoc Neurosci* 2007. Chapter 8: pp. Unit 8.9.

Barcena de Arellano ML, Arnold J, Lang H, Vercellino GF, Chiantera V, Schneider A, Mechsner S. Evidence of neurotrophic events due to peritoneal endometriotic lesions. *Cytokine* 2013;**62**:253–261.

Barcena de Arellano ML, Arnold J, Vercellino GF, Chiantera V, Ebert AD, Schneider A, Mechsner S. Influence of nerve growth factor in endometriosis-associated symptoms. *Reprod Sci* 2011;**18**:1202–1210.

Bergqvist A, Nejaty H, Froysa B, Bruse C, Carlberg M, Sjoblom P, Soder O. Production of interleukins 1beta, 6 and 8 and tumor necrosis factor alpha in separated and cultured endometrial and endometriotic stromal and epithelial cells. *Gynecol Obstet Invest* 2000;**50**:1–6.

Berkley KJ, Dmitrieva N, Curtis KS, Papka RE. Innervation of ectopic endometrium in a rat model of endometriosis. *Proc Natl Acad Sci USA* 2004;**101**:11094–11098.

Cassidy MR, Sheldon HK, Gainsbury ML, Gillespie E, Kosaka H, Heydrick S, Stucchi AF. The neurokinin 1 receptor regulates peritoneal fibrinolytic activity and postoperative adhesion formation. *J Surg Res* 2014;**191**:12–18.

Chichger H, Vang A, O'Connell KA, Zhang P, Mende U, Harrington EO, Choudhary G. PKC δ and βII regulate angiotensin II-mediated fibrosis through p38: a mechanism of RV fibrosisin pulmonary hypertension. *Am J Physiol Lung Cell Mol Physiol* 2015;**308**:L827–L836.

Ding D, Liu X, Duan J, Guo SW. Platelets are an unindicted culprit in the development of endometriosis: clinical and experimental evidence. *Hum Reprod* 2015;**30**:812–832.

Doltra A, Messroghli D, Stawowy P, Hassel JH, Gebker R, Leppanen O, Grafe M, Schneeweis C, Schnackenburg B, Fleck E *et al*. Potential reduction of interstitial myocardial fibrosis with renal denervation. *J Am Heart Assoc* 2014;**3**:e001353.

Duan J, Liu X, Wang H, Guo SW. The M2a macrophage subset may be critically involved in the fibrogenesis of endometriosis in mice. *Reprod Biomed Online* 2018;**37**:254–268.

Eliav E, Benoliel R, Herzberg U, Kalladka M, Tal M. The role of IL-6 and IL-1beta in painful perineural inflammatory neuritis. *Brain Behav Immun* 2009;**23**:474–484.

Engin C, Demirkan F, Ayhan S, Atabay K, Baran NK. Delayed effect of denervation on wound contraction in rat skin. *Plast Reconstr Surg* 1996;**98**:1063–1067.

Esposito AJ, Heydrick SJ, Cassidy MR, Gallant J, Stucchi AF, Becker JM. Substance P is an early mediator of peritoneal fibrinolytic pathway genes and promotes intra-abdominal adhesion formation. *J Surg Res* 2013;**181**:25–31.

Ferrero S, Alessandri F, Racca A, Leone Roberti Maggiore U. Treatment of pain associated with deep endometriosis: alternatives and evidence. *Fertil Steril* 2015;**104**:771–792.

Ferrero S, Haas S, Remorgida V, Camerini G, Fulcheri E, Ragni N, Straub RH, Capellino S. Loss of sympathetic nerve fibers in intestinal endometriosis. *Fertil Steril* 2010;**94**:2817–2819.

Foldenauer ME, McClellan SA, Barrett RP, Zhang Y, Hazlett LD. Substance P affects growth factors in Pseudomonas aeruginosa-infected mouse cornea. *Cornea* 2012;**31**:1176–1188.

Garcia-Recio S, Gascón P. Biological and pharmacological aspects of the NK1-receptor. *Biomed Res Int* 2015;**2015**:495704.

Gerard NP, Garraway LA, Eddy RL Jr., Shows TB, Iijima H, Paquet JL, Gerard C. Human substance P receptor (NK-1): organization of the gene, chromosome localization, and functional expression of cDNA clones. *Biochemistry* 1991;**30**:10640–10646.

Gibbins JM. Tweaking the gain on platelet regulation: the tachykinin connection. *Atherosclerosis* 2009;**206**:1–7.

Giudice LC, Kao LC. Endometriosis. *Lancet* 2004;**364**:1789–1799.

Gonzalez-Ramos R, Van Langendonckt A, Defrere S, Lousse JC, Colette S, Devoto L, Donnez J. Involvement of the nuclear factor-kappaB pathway in the pathogenesis of endometriosis. *Fertil Steril* 2010;**94**:1985–1994.

Gosain A, Jones SB, Shankar R, Gamelli RL, DiPietro LA. Norepinephrine modulates the inflammatory and proliferative phases of wound healing. *J Trauma* 2006;**60**:736–744.

Graham GJ, Stevens JM, Page NM, Grant AD, Brain SD, Lowry PJ, Gibbins JM. Tachykinins regulate the function of platelets. *Blood* 2004;**104**:1058–1065.

Guide for the Care and Use of Laboratory Animals. 2011, Washington, DC.

Guo SW. Nuclear factor-kappab (NF-kappaB): an unsuspected major culprit in the pathogenesis of endometriosis that is still at large? *Gynecol Obstet Invest* 2007;**63**:71–97.

He W, Liu X, Zhang Y, Guo SW. Generalized hyperalgesia in women with endometriosis and its resolution following a successful surgery. *Reprod Sci* 2010;**17**:1099–1111.

Hsiao TH, Fu YS, Ho WY, Chen TH, Hsieh YL. Promotion of thermal analgesia and neuropeptidergic skin reinnervation by 4-methylcatechol in resiniferatoxin-induced neuropathy. *Kaohsiung J Med Sci* 2013;**29**:405–411.

Hsieh YL, Chiang H, Tseng TJ, Hsieh ST. Enhancement of cutaneous nerve regeneration by 4-methylcatechol in resiniferatoxin-induced neuropathy. *J Neuropathol Exp Neurol* 2008;**67**:93–104.

Jenkins S, Olive DL, Haney AF. Endometriosis: pathogenetic implications of the anatomic distribution. *Obstet Gynecol* 1986;**67**:335–338.

Jiang MH, Chung E, Chi GF, Ahn W, Lim JE, Hong HS, Kim DW, Choi H, Kim J, Son Y. Substance P induces M2-type macrophages after spinal cord injury. *Neuroreport* 2012;**23**:786–792.

Jones S, Gibbins JM. The neurokinin 1 receptor: a potential new target for anti-platelet therapy? *Curr Opin Pharmacol* 2008;**8**:114–119.

Jones S, Tucker KL, Sage T, Kaiser WJ, Barrett NE, Lowry PJ, Zimmer A, Hunt SP, Emerson M, Gibbins JM. Peripheral tachykinins and the neurokinin receptor NK1 are required for platelet thrombus formation. *Blood* 2008;**111**:605–612.

Kanai S, Ishihara K, Kawashita E, Tomoo T, Nagahira K, Hayashi Y, Akiba S. ASB14780, an orally active inhibitor of group IVA phospholipase A2, is a pharmacotherapeutic candidate for nonalcoholic fatty liver disease. *J Pharmacol Exp Ther* 2016;**356**:604–614.

Kant V, Kumar D, Kumar D, Prasad R, Gopal A, Pathak NN, Kumar P, Tandan SK. Topical application of substance P promotes wound healing in streptozotocin-induced diabetic rats. *Cytokine* 2015;**73**:144–155.

Karai L, Brown DC, Mannes AJ, Connelly ST, Brown J, Gandal M, Wellisch OM, Neubert JK, Olah Z, Iadarola MJ. Deletion of vanilloid receptor 1-expressing primary afferent neurons for pain control. *J Clin Invest* 2004;**113**:1344–1352.

Khan MM, Douglas SD, Benton TD. Substance P-neurokinin-1 receptor interaction upregulates monocyte tissue factor. *J Neuroimmunol* 2012;**242**:1–8.

Koninckx PR, Martin DC. Deep endometriosis: a consequence of infiltration or retraction or possibly adenomyosis externa? *Fertil Steril* 1992;**58**:924–928.

Koninckx PR, Ussia A, Adamyan L, Wattiez A, Donnez J. Deep endometriosis: definition, diagnosis, and treatment. *Fertil Steril* 2012;**98**:564–571.

Koon HW, Zhao D, Zhan Y, Rhee SH, Moyer MP, Pothoulakis C. Substance P stimulates cyclooxygenase-2 and prostaglandin E2 expression through JAK-STAT activation in human colonic epithelial cells. *J Immunol* 2006;**176**:5050–5059.

Kruszewska B, Felten DL, Stevens SY, Moynihan JA. Sympathectomy-induced immune changes are not abrogated by the glucocorticoid receptor blocker RU-486. *Brain Behav Immun* 1998;**12**:181–200.

Kuligowska E, Deeds L 3rd, Lu K 3rd. Pelvic pain: overlooked and underdiagnosed gynecologic conditions. *Radiographics* 2005;**25**:3–20.

Kwon YB, Yoon SY, Kim HW, Roh DH, Kang SY, Ryu YH, Choi SM, Han HJ, Lee HJ, Kim KW *et al*. Substantial role of locus coeruleus-noradrenergic activation and capsaicin-insensitive primary afferent fibers in bee venom's anti-inflammatory effect. *Neurosci Res* 2006;**55**:197–203.

Lai JP, Lai S, Tuluc F, Tansky MF, Kilpatrick LE, Leeman SE, Douglas SD. Differences in the length of the carboxyl terminus mediate functional properties of neurokinin-1 receptor. *Proc Natl Acad Sci USA* 2008;**105**:12605–12610.

Leal EC, Carvalho E, Tellechea A, Kafanas A, Tecilazich F, Kearney C, Kuchibhotla S, Auster ME, Kokkotou E, Mooney DJ *et al*. Substance P promotes wound healing in diabetes by modulating inflammation and macrophage phenotype. *Am J Pathol* 2015;**185**:1638–1648.

Lei X, Li Q, Rodriguez S, Tan SY, Seldin MM, McLenithan JC, Jia W, Wong GW. Thromboxane synthase deficiency improves insulin action and attenuates adipose tissue fibrosis. *Am J Physiol Endocrinol Metab* 2015;**308**:E792–E804.

Liang Y, Wang W, Huang J, Tan H, Liu T, Shang C, Liu D, Guo L, Yao S. Potential role of semaphorin 3A and its receptors in regulating aberrant sympathetic innervation in peritoneal and deep infiltrating endometriosis. *PLoS One* 2015;**10**:e0146027.

Lim JE, Chung E, Son Y. A neuropeptide, Substance-P, directly induces tissue-repairing M2 like macrophages by activating the PI3K/Akt/mTOR pathway even in the presence of IFNgamma. *Sci Rep* 2017;**7**:9417.

Liu M, Ning X, Li R, Yang Z, Yang X, Sun S, Qian Q. Signalling pathways involved in hypoxia-induced renal fibrosis. *J Cell Mol Med* 2017;**21**:1248–1259.

Liu X, Shen M, Qi Q, Zhang H, Guo SW. Corroborating evidence for platelet-induced epithelial-mesenchymal transition and fibroblast-to-myofibroblast transdifferentiation in the development of adenomyosis. *Hum Reprod (Oxford, England)* 2016;**31**:734–749.

Liu X, Zhang Q, Guo S-W. Histological and immunohistochemical characterization of the similarity and difference between ovarian endometriomas and deep infiltrating endometriosis. *Reprod Sci* 2018;**25**:329–340.

Liu Q, Zhang Q, Wang K, Wang S, Lu D, Li Z, Geng J, Fang P, Wang Y, Shan Q. Renal denervation findings on cardiac and renal fibrosis in rats with isoproterenol induced cardiomyopathy. *Sci Rep* 2015;**5**:18582.

Long Q, Liu X, Guo SW. Surgery accelerates the development of endometriosis in mouse. *Am J Obstet Gynecol* 2016;**215**:320.e1–320.e15.

Lu Y, Nie J, Liu X, Zheng Y, Guo SW. Trichostatin A, a histone deacetylase inhibitor, reduces lesion growth and hyperalgesia in experimentally induced endometriosis in mice. *Hum Reprod* 2010;**25**:1014–1025.

Lu W, Yao X, Ouyang P, Dong N, Wu D, Jiang X, Wu Z., Zhang C., Xu Z., Tang X *et al*. Drug repurposing of histone deacetylase inhibitors that alleviate neutrophilic inflammation in acute lung injury and idiopathic pulmonary fibrosis via inhibiting leukotriene A4 hydrolase and blocking LTB4 biosynthesis. *J Med Chem* 2017;**60**:1817–1828.

Luedde T, Schwabe RF. NF-κB in the liver—linking injury, fibrosis and hepatocellular carcinoma. *Nat Rev Gastroenterol Hepatol* 2011;**8**:108–118.

Mathias JR, Clench MH, Davis RH, Sninsky CA, Pineiro-Carrero VM. Migrating action potential complex: unmasked by 6-hydroxydopamine. *Am J Physiol* 1985;**249**:G416–G421.

McKinnon B, Bersinger NA, Wotzkow C, Mueller MD. Endometriosis-associated nerve fibers, peritoneal fluid cytokine concentrations, and pain in endometriotic lesions from different locations. *Fertil Steril* 2012;**97**:373–380.

McKinnon BD, Evers J, Bersinger NA, Mueller MD. Induction of the neurokinin 1 receptor by TNFalpha in endometriotic tissue provides the potential for neurogenic control over endometriotic lesion growth. *J Clin Endocrinol Metab* 2013;**98**:2469–2477.

Mechsner S, Kaiser A, Kopf A, Gericke C, Ebert A, Bartley J. A pilot study to evaluate the clinical relevance of endometriosis-associated nerve fibers in peritoneal endometriotic lesions. *Fertil Steril* 2009;**92**:1856–1861.

Mechsner S, Schwarz J, Thode J, Loddenkemper C, Salomon DS, Ebert AD. Growth-associated protein 43-positive sensory nerve fibers accompanied by immature vessels are located in or near peritoneal endometriotic lesions. *Fertil Steril* 2007;**88**:581–587.

Nanji AA, Liong EC, Xiao J, Tipoe GL. Thromboxane inhibitors attenuate inflammatory and fibrotic changes in rat liver despite continued ethanol administrations. *Alcohol Clin Exp Res* 2013;**37**:31–39.

Neubert JK, Karai L, Jun JH, Kim HS, Olah Z, Iadarola MJ. Peripherally induced resiniferatoxin analgesia. *Pain* 2003;**104**:219–228.

Nisolle M, Donnez J. Peritoneal endometriosis, ovarian endometriosis, and adenomyotic nodules of the rectovaginal septum are three different entities. *Fertil Steril* 1997;**68**:585–596.

Page NM, Bell NJ, Gardiner SM, Manyonda IT, Brayley KJ, Strange PG, Lowry PJ. Characterization of the endokinins: human tachykinins with cardiovascular activity. *Proc Natl Acad Sci USA* 2003;**100**:6245–6250.

Perez MC, Bodine PV, Leiva MC, Isaacson KB, Komm BS. Signal transduction pathways involved in macrophage migration induced by peritoneal fluid chemotactic factors in stages I and II endometriosis. *Fertil Steril* 2002;**77**:1261–1268.

R Core Team. *R: A Language and Environment for Statistical Computing*. Vienna, Austria: R Foundation for Statistical Computing, 2018.

Richards AM, Floyd DC, Terenghi G, McGrouther DA. Cellular changes in denervated tissue during wound healing in a rat model. *Br J Dermatol* 1999;**140**:1093–1099.

Shu B, Xie JL, Xu YB, Lai W, Huang Y, Mao RX, Liu XS, Qi SH. Effects of skin-derived precursors on wound healing of denervated skin in a nude mouse model. *Int J Clin Exp Pathol* 2015;**8**:2660–2669.

Singh S, Natarajan K, Aggarwal BB. Capsaicin (8-methyl-N-vanillyl-6-nonenamide) is a potent inhibitor of nuclear transcription factor-kappa B activation by diverse agents. *J Immunol* 1996;**157**:4412–4420.

Smith PG, Liu M. Impaired cutaneous wound healing after sensory denervation in developing rats: effects on cell proliferation and apoptosis. *Cell Tissue Res* 2002;**307**:281–291.

Somigliana E, Vigano P, Rossi G, Carinelli S, Vignali M, Panina-Bordignon P. Endometrial ability to implant in ectopic sites can be prevented by interleukin-12 in a murine model of endometriosis. *Hum Reprod* 1999;**14**:2944–2950.

Steinhoff MS, von Mentzer B, Geppetti P, Pothoulakis C, Bunnett NW. Tachykinins and their receptors: contributions to physiological control and the mechanisms of disease. *Physiol Rev* 2014;**94**:265–301.

Tattersall FD, Rycroft W, Cumberbatch M, Mason G, Tye S, Williamson DJ, Hale JJ, Mills SG, Finke PE, MacCoss M *et al*. The novel NK1 receptor antagonist MK-0869 (L-754,030) and its water soluble phosphoryl prodrug, L-758,298, inhibit acute and delayed cisplatin-induced emesis in ferrets. *Neuropharmacology* 2000;**39**:652–663.

Tokushige N, Markham R, Russell P, Fraser IS. Nerve fibres in peritoneal endometriosis. *Hum Reprod* 2006;**21**:3001–3007.

Tosti C, Pinzauti S, Santulli P, Chapron C, Petraglia F. Pathogenetic mechanisms of deep infiltrating endometriosis. *Reprod Sci* 2015.

Vaughan CH, Zarebidaki E, Ehlen JC, Bartness TJ. Analysis and measurement of the sympathetic and sensory innervation of white and brown adipose tissue. *Methods Enzymol* 2014;**537**:199–225.

Wang K, Lu D, Zhang B, Wang S, Liu Q, Zhang Q, Geng J, Shan Q. Renal denervation attenuates multi-organ fibrosis and improves vascular

remodeling in rats with transverse aortic constriction induced cardiomyopathy. *Cell Physiol Biochem* 2016;**40**:465–476.

Wang G, Tokushige N, Markham R, Fraser IS. Rich innervation of deep infiltrating endometriosis. *Hum Reprod* 2009;**24**:827–834.

Xiao L, Kirabo A, Wu J, Saleh MA, Zhu L, Wang F, Takahashi T, Loperena R, Foss JD, Mernaugh RL *et al*. Renal denervation prevents immune cell activation and renal inflammation in Angiotensin II-induced hypertension. *Circ Res* 2015;**117**:547–557.

Yamaguchi R, Yamamoto T, Sakamoto A, Ishimaru Y, Narahara S, Sugiuchi H, Yamaguchi Y. Substance P enhances tissue factor release from granulocyte-macrophage colony-stimulating factor-dependent macrophages via the p22phox/beta-arrestin 2/Rho A signaling pathway. *Blood Cells Mol Dis* 2016;**57**:85–90.

Yan D, Liu X, Guo SW. Endometriosis-derived thromboxane A2 induces neurite outgrowth. *Reprod Sci* 2017;**24**:829–835.

Yang L, Di G, Qi X, Qu M, Wang Y, Duan H, Danielson P, Xie L, Zhou Q. Substance P promotes diabetic corneal epithelial wound healing through molecular mechanisms mediated via the neurokinin-1 receptor. *Diabetes* 2014;**63**:4262–4274.

Zamah NM, Dodson MG, Stephens LC, Buttram VC Jr., Besch PK, Kaufman RH. Transplantation of normal and ectopic human endometrial tissue into athymic nude mice. *Am J Obstet Gynecol* 1984;**149**:591–597.

Zhang Q, Duan J, Liu X, Guo SW. Platelets drive smooth muscle metaplasia and fibrogenesis in endometriosis through epithelial-mesenchymal transition and fibroblast-to-myofibroblast transdifferentiation. *Mol Cell Endocrinol* 2016a;**428**:1–16.

Zhang Q, Duan J, Olson M, Fazleabas A, Guo SW. Cellular changes consistent with epithelial-mesenchymal transition and fibroblast-to-myofibroblast transdifferentiation in the progression of experimental endometriosis in baboons. *Reprod Sci* 2016b;**23**:1409–1421.

Zhang Q, Liu X, Guo SW. Progressive development of endometriosis and its hindrance by anti-platelet treatment in mice with induced endometriosis. *Reprod Biomed Online* 2017;**34**:225–239.